1

Mechanisms and feedbacks causing changes in upper stratospheric ozone in the 21st century

L. Oman[1], D.W. Waugh[1], S.R. Kawa[2], R. S. Stolarski[2],
A.R. Douglass[2], P.A. Newman[2]

[1]Department of Earth and Planetary Sciences, Johns Hopkins University, Baltimore, Maryland
[2]Atmospheric Chemistry and Dynamics Branch, NASA Goddard Space Flight Center, Greenbelt, Maryland

Corresponding Author:
Luke Oman
Department of Earth and Planetary Sciences
Johns Hopkins University
301 Olin Building
3400 North Charles Street
Baltimore, MD 21218
Email: oman@jhu.edu

Popular Summary:

Driving forces behind 21st century ozone evolution

One of the important science questions that need to be address is concerning how ozone will evolve in the future and what factors are causes this change. Ozone is a very important atmospheric gas that absorbs damaging ultraviolet radiation, so changes in the total amount above us can have important consequences for our biosphere. The ability of ozone to absorb sunlight, mainly in the ultraviolet but also some in the visible range, as well as some of Earth's outgoing longwave radiation causes heating of the upper layers of our atmosphere which can have many impacts, including changing the winds.

A new study by scientists at NASA's Goddard Space Flight Center (GSFC) and Johns Hopkins University used a state-of-the-art chemistry climate model to explain what could potentially be driving changes in ozone in the upper levels of our atmosphere over the 21st century. They found that in the upper stratosphere, the region from 20 to 30 miles above the surface, the reduction in chlorine and cooling temperatures contribute about equally to future increases in ozone in the tropics. The future reduction in chlorine, which is formed mostly from the breakdown of chlorofluorocarbons (CFC's), is the expected result of the successful implementation of the Montreal Protocol and its subsequent amendments and adjustments. The continued cooling of the stratosphere is a response largely caused by increasing concentrations of carbon dioxide (CO_2), which is opposite of the warming that CO_2 causes closer to the surface.

The technique that was developed in this study helps to separate the relative contributions of several factors that can influence ozone and can be applied to a wide range of greenhouse gas scenarios as well as to other chemistry climate models. This method can potentially be very useful in explaining differences in ozone trends among models and will be used in an upcoming assessment for this purpose. This work is part of a larger chemistry climate project at GSFC with the ultimate goal of using observations and computer modeling to improve our knowledge of Earth's climate system.
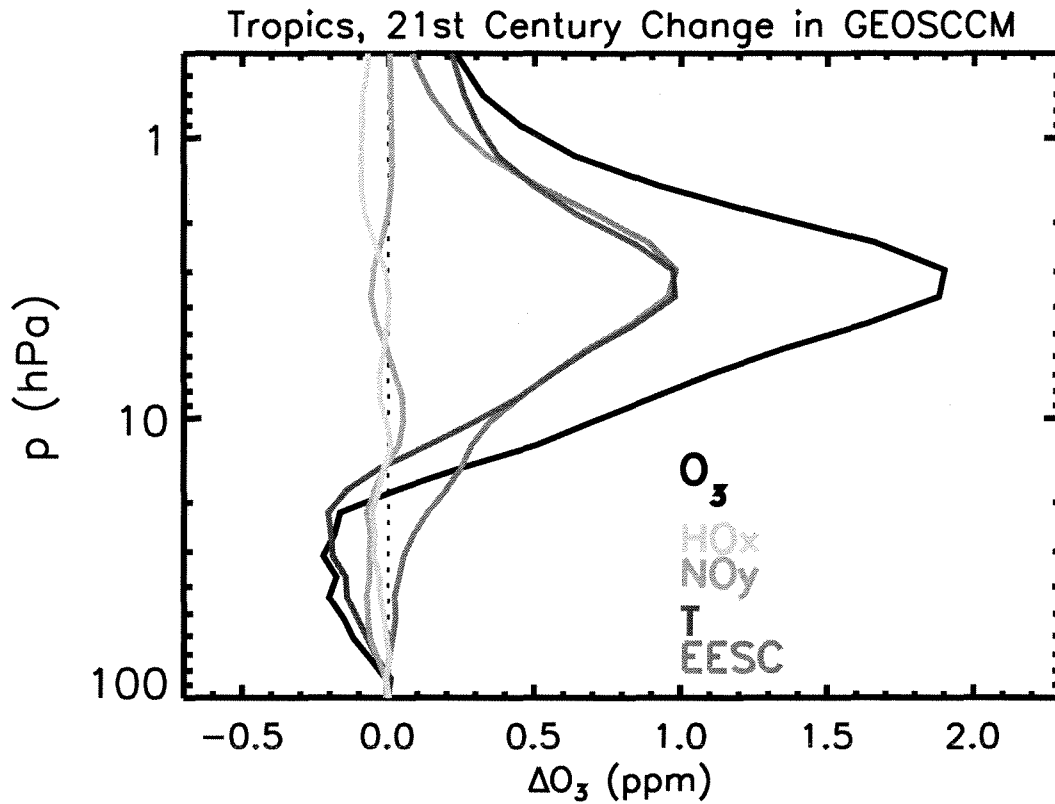
Relevant image:

Figure caption: Vertical variation of trends in ozone (solid black curve) and individual contribution of different mechanisms over the tropics (10°S-10°N) for the 21st century in GEOSCCM. The dominate impacts are from temperature (T, blue curve) changes and chlorine (EESC, red curve) changes with negligable contribution from hydrogen (HO$_x$, green curve) and nitrogen (NO$_y$, orange curve) oxides for the A1b (mid-range) greenhouse gas scenario.

47

Abstract

49   Stratospheric ozone is expected to increase during the 21st century as the

50 abundance of halogenated ozone-depleting substances decrease to 1960 values.

51 However, climate change will likely alter this "recovery" of stratospheric ozone by

52 changing stratospheric temperatures, circulation, and abundance of reactive chemical

53 species. Here we quantify the contribution of different mechanisms to changes in upper

54 stratospheric ozone from 1960 to 2100 in the Goddard Earth Observing System

55 Chemistry-Climate Model (GEOS CCM), using multiple linear regression analysis

56 applied to simulations using either A1b or A2 greenhouse gas (GHG) scenarios. In both

57 these scenarios upper stratospheric ozone has a secular increase over the 21st century. For

58 the simulation using the A1b GHG scenario, this increase is determined by the decrease

59 in halogen amounts and the greenhouse gas induced cooling, with roughly equal

60 contributions from each mechanism. There is a larger cooling in the simulation using the

61 A2 GHG scenario, but also enhanced loss from higher NO_y and HO_x concentrations,

62 which nearly offsets the increase due to cooler temperatures. The resulting ozone

63 evolutions are similar in the A2 and A1b simulations. The response of ozone due to

64 feedbacks from temperature and HO_x changes, related to changing halogen

65 concentrations, are also quantified using simulations with fixed halogen concentrations.

66

1 Introduction

68

69   One of the critical questions of Earth's climate system is how ozone

70   concentrations will evolve during the 21st century. The concentration of ozone-depleting

71   substances (ODS) increased rapidly during the 1960s to 1980s, peaked in 1990s, and is

72   expected to decrease almost back to 1960s levels by the end of this century. As the

73   abundance of stratospheric halogens returns to 1960s values, stratospheric ozone, if there

74   were no other changes, would be expected to increase back to 1960s values. However,

75   the concentrations of greenhouse gases (GHGs) are expected to continue to increase,

76   causing other changes in the thermal, dynamical, and chemical structure of the

77   stratosphere. These changes could alter the "expected" recovery of stratospheric ozone by

78   a variety of mechanisms. For example, the upper stratosphere is expected to continue to

79   cool due to the continued increase of CO_2. This cooling will slow the rate of gas-phase

80   reactions that destroy ozone, and hence increase ozone concentrations [e.g., *Haigh and*

81   *Pyle*, 1979; *Brasseur and Hitchman*, 1988, *Shindell et al.*, 1998; *Rosenfield et al.*, 2002].

82   Increases in N_2O and CH_4 could also impact the recovery of ozone by increasing nitrogen

83   and hydrogen ozone-loss cycles [e.g., *Randeniya et al.*, 2002; *Rosenfield et al.*, 2002;

84   *Chipperfield and Feng*, 2003; *Portmann and Solomon*, 2007]. Increases in GHGs have

85   also been linked to changes in stratospheric transport that could impact the ozone

86   recovery [*Waugh et al.*, 2009; *Li et al.*, 2009].

87   Projections of the ozone evolution in the 21st century use models that couple

88   stratospheric chemistry and climate. Until *WMO* [2007] global ozone projections were

89   made primarily with two-dimensional (2D) models, most of which did not include

90   coupling between future temperature changes and the chemistry. Some projections were

91   made with 2D models including this coupling [e.g., *Rosenfield et al.*, 2002; *Chipperfield*

92   *and Feng*, 2003; *Portmann and Solomon*, 2007], however these models did not fully

93   capture circulation changes due to changes in wave driving from the troposphere or

94   changes in the polar vortices.   More recently, three-dimensional models that include full

95   representations of dynamical, radiative, and chemical processes in the atmosphere, and

96   the couplings between these processes, have been developed, and these "chemistry-

97   climate models" (CCMs) have been used to make projections of ozone through the 21st

98   century [e.g. *Austin and Wilson*, 2006; *Eyring et al.*, 2007; *Shepherd*, 2008].

99   While there have been detailed analyses of the simulated ozone in these CCMs

100 there has been rather limited quantitative attribution of these ozone changes to the

101 different mechanisms.   Although several studies have attributed increases in upper

102 stratospheric ozone and decreases in lower stratosphere ozone to cooling and circulation

103 changes respectively [e.g., *Eyring et al.*, 2007; *Shepherd*, 2008; *Li et al.*, 2009], the

104 relative role of the different mechanisms has not been quantified.   *Newchurch* et al.

105 [2003] examined 10 years of HALOE observations to attribute changes in ozone to

106 different mechanisms, however it was limited by the time period and available

107 observations of trace gases. Quantitative attribution has been performed for some CCMs

108 with simulations using either fixed GHGs [e.g., *WMO*, 2007] or fixed ODSs [e.g., *Waugh*

109 *et al.*, 2009].   However, such analysis does not isolate the relative role of different GHG-

110 related mechanisms in causing changes in ozone. This attribution is needed to understand

111 exactly how changes in different GHGs will impact stratospheric ozone. There are often

112 multiple mechanisms by which an increase in a GHG can impact ozone, and the sign of

113 the ozone changes are not necessarily the same for each mechanism. Without knowledge

114 of the relative role of different mechanisms it is difficult to know how ozone projections

115   will change for different GHG scenarios (e.g., whether the GHG impact on ozone will

116   simply scale with GHG concentrations).   This is important as the recent CCM

117   projections of the 21st century have all used the same GHG scenario [*Eyring et al.*, 2007],

118   and there have not been comparisons of projections for different scenarios (other than the

119   unrealistic case of fixed GHGs).

120

121   Here we use multiple linear regression (MLR) to estimate the relative contribution of

122   changes in halogens, temperature, reactive nitrogen (NO_y), and reactive hydrogen (HO_x)

123   to changes in the simulated ozone from the NASA Goddard Earth Observing System

124   Chemistry-Climate Model (GEOS CCM) [*Pawson et al.*, 2008]. We consider simulations

125   using two different scenarios of future GHG emissions: The IPCC (2001) A1b scenario

126   that has been used in most recent CCM simulations and the A2 scenario which has larger

127   increases in all GHGs.   Even though there are significant differences in the GHG

128   concentrations in the latter half of the 21st century, the ozone changes in these two

129   simulations are very similar.   The MLR indicates that the net changes in upper

130   stratospheric ozone are similar because of the compensating effects of larger cooling and

131   larger abundances of reactive nitrogen and hydrogen in the simulation with larger GHGs

132   changes.

133

134   The model, simulations and evolution of ozone in the GEOS CCM simulations are

135   described in the next Section. The simulated changes in ozone and quantities that can

136   impact ozone are described in Section 3.   Methods used in the analysis are presented in

137   Section 4. Then in Section 5 we quantify the relative contribution of different

138   mechanisms to ozone changes in the upper stratosphere. Section 6 compares the results to

139   a fixed halogen simulation and concluding remarks are given in Section 7.

140

141

142   ## 2 Model

143

144

145   We consider here GEOS CCM [*Pawson et al.*, 2008] simulations of the past (1960-2004)

146   and future (2000-2100). The past simulations use the observed Hadley sea surface

147   temperatures (SST) and sea ice data set from *Rayner et al.* [2003], while the future

148   simulations use SST and sea ice data from AR4 integrations of the NCAR Community

149   Climate System Model, version 3 (CCSM3) for both the *IPCC* [2001] A1b or A2 GHG

150   scenario. Observed surface concentrations of GHGs and halogens are used for past

151   simulations. Future simulations use the A1b or A2 scenario for surface concentrations of

152   GHGs and the *WMO* [2003] Ab scenario for surface concentrations of halogens. The

153   time series of the surface concentrations of the GHGs and total chlorine, normalized by

154   their 1960 values, are shown in Figure 1a. The two GHG scenarios are fairly similar until

155   about 2040, when the A2 scenario shows faster increases of CO_2 and N_2O. CH_4

156   continues to increase in this scenario whereas it peaks around 2050 in the A1b scenario.

157   Comparisons of the simulated temperature, ozone, water vapor, and other

158   constituents with observations have been discussed in *Pawson et al.* [2008], *Eyring et al.*

159   [2006, 2007], and *Oman et al.* [2008]. These studies have shown that GEOS CCM

160   performs reasonably well compared to observations. Two noted deficiencies are a high

161   bias in total O_3 at high latitudes when chlorine loading is low (in the 1960s) and the late

162   break up of the Antarctic polar vortex [*Pawson et al.*, 2008].

163   There is a 5 year overlap (2000-2004) in the above two simulations. In the

164   analysis presented below we join the simulations together in January 2001 to form a

165   single time series from January 1960 to December 2099. We use "A1b" to denote the

166   combination of the first reference past simulation (P1) and the A1b future simulation, and

167   "A2" for the combination of the second reference past (P2) and A2 future simulation.

168   The P2 simulation is a second ensemble member of P1, varying only in initial conditions

169   [*Oman et al.*, 2009]. A small discontinuity at January 2001, apparent in the time series

170   for some quantities at some locations, does not impact results presented here. Below

171   when we refer to a single simulation we are referring to the composite past and future

172   simulations joined in January 2001.

173

174

175   **3 Modeled Changes 1960 to 2100**

176

177   Before examining the mechanisms responsible for ozone changes, we examine the

178   changes in ozone and the quantities that can impact ozone changes in the GEOS CCM

179   simulations, focusing on the long-term changes between 1960 and 2100 for the two

180   simulations. Evolution of the 60°S-60°N average total column ozone and the partial

181   columns above and below 20 hPa is similar for the A1b (solid) and A2 (dashed)

182   simulations (Figure 1b).

183   In both, column ozone (black curves) decreases from 1960 to around 2000, and

184   then increases back to values similar to 1960 in 2100. This evolution of total column

185   ozone is qualitatively similar to that of the negative of the tropospheric total chlorine (see

186   Figure 1a), except the total chlorine peaks a few years earlier and has not quite returned

187   to 1960 values by 2100. Although the extra-polar total column ozone in 2100 is similar

188   to that in 1960s this is not necessarily the case for the ozone mixing ratio at a given

189   location. In general, upper stratospheric ozone in the 2090s exceeds the 1960s values

190   whereas the opposite is true for lower stratospheric ozone. This can be seen in the

191   evolution of partial columns of ozone above and below 20 hPa, see Figure 1b (note that

192   80 DU was added to partial column above 20 hPa for graphical purposes).

193   Further details of the differences in long-term evolution are shown in Figures 2a

194   and b, which show the change in decadal-averaged ozone between 1960s and 2090s for

195   the (a) A1b and (b) A2 simulations. Here, and below, "1960s" ozone refers to the ozone

196   averaged over the years 1960 to 1969, and "2090s" ozone is the average from 2090 to

197   2099. These plots show that in both simulations the decadal-averaged 2090s extra-polar

198   ozone is larger than that in the 1960s in the upper stratosphere, similar to 1960s in the

199   mid stratosphere, and less than 1960s in the lower stratosphere.

200   As discussed in the Introduction, a number of mechanisms can influence the

201   evolution of ozone concentrations in the stratosphere. To help understand the changes in

202   ozone between the 1960s and 2090s we show in Figures 2c-l the change between 1960s

203   and 2090s in several quantities that influence ozone. As shown in Figures 2c and d,

204   equivalent effective stratospheric chlorine ("EESC"; where $EESC = Cl_y + \alpha\, Br_y$, with

205    $\alpha = 5$) in 2090s has returned to values similar to those in the 1960s in the lower

206   stratosphere, and is only around than 0.3 to 0.4 ppb larger in the upper stratosphere

207   (compare to the peak EESC values of around 3-4 ppb in 2000). (We use α = 5 in the

208   definition as *Daniel et al.* [1999] show this is an appropriate value for the upper

209   stratosphere, which is the focus of this study.) As a result, changes in EESC only make a

210   minor contribution to the 1960 to 2100 changes in ozone (see below). This is not

211   necessarily the case, however, for temperature, NO_y, HO_x, and residual vertical velocity.

212   In both simulations there is stratospheric cooling (Figures 2e,f), associated primarily with

213   increasing concentrations of GHGs. The A2 simulation shows the largest cooling

214   consistent with the higher GHG concentrations in this scenario (cf., Figure 1a). This

215   larger cooling in the A2 simulation alone causes slower destruction of ozone and larger

216   increase in ozone compared to the A1b simulation. However, as discussed above, the net

217   ozone is similar in the A1b and A2 simulations implying that other compensating

218   changes in ozone are occurring.

219   Two other mechanisms for changes in ozone concentrations are changes in

220   nitrogen and hydrogen ozone-loss cycles. Figures 2g-j shows that the magnitude of

221   changes in NO_y and HO_x between 1960s and 2090s are different in the A1b and A2

222   simulations, with a larger increase in upper stratospheric NO_y and HO_x in the A2

223   simulation (again, consistent with higher GHG concentrations in this scenario, see Figure

224   1a). It is important to note that changes in HO_x and NO_y do not simply follow changes in

225   CH_4 and N_2O, respectively. This can be seen by comparing Figures 2g,i with Figure 1a:

226   There are negative changes in some areas in NO_y and HO_x from 1960s-2090s despite

227   large increases in N_2O and CH_4. The difference between HO_x and CH_4 trends is because

228   methane oxidation is not the only source of stratospheric H_2O, changes in the tropical

229   tropopause cold point also influence stratospheric H_2O [See *Oman et al.,* 2008]. HO_x

230 formation can be influenced additionally by changes in ultra-violet radiation and ozone

231 concentration. NO_y - N_2O trend differences occur because the loss of NO_y is influenced

232 by temperature [*Rosenfield and Douglass*, 1998] and also could be affected by circulation

233 changes.

234 Changes in transport also influence the ozone evolution, and Figures 2k and l

235 show the change in residual vertical velocity, as a proxy for circulation changes. There is

236 a similar increase in the tropical vertical velocity between the 1960s and 2090s in the two

237 simulations, with a slightly larger change in the A2 simulation.

238 In summary, Figure 2 shows that there are larger changes in temperature, NO_y,

239 and HO_x in the A2 simulation, but the ozone change is similar in the two simulations.

240 This suggests compensating ozone changes due to different mechanisms, which is

241 quantified below.

242

243

244 **4 Linear Regression Analysis**

245

246 We wish to estimate the contribution of the different mechanisms to the simulated

247 changes in ozone. The principal analysis method used to do this is multiple linear

248 regression (MLR). For a given location and time, MLR is applied to determine the

249 coefficients m_X such that

250
$$\Delta O_3(t) = \sum_j m_{X_j} \Delta X_j(t) + \varepsilon(t),$$
(1)

251 where the X_j are the different quantities that could influence ozone, the coefficients m_X

252 are the sensitivity of ozone to the quantity X, i.e., $m_X = \partial O_3 / \partial X$, and ε is the error in the

253 fit. MLR analysis has been extensively applied to observations or simulations to isolate

254 a long-term linear trend in ozone (and more recently long-term variations in ozone

255 correlated with EESC) (e.g. *WMO* [2007] and references therein).

256 To apply equation (1) we need to decide which mechanisms we wish to isolate,

257 and the quantities X_j that are the "proxies" for these different mechanisms. In the MLR

258 calculations presented below we focus on ozone-changes due to changes in halogen,

259 nitrogen, and hydrogen ozone-loss cycles as well as changes in temperature. To do this

260 four explanatory variables (X_j) are used in (1): EESC, reactive nitrogen (NO_y =

261 $NO+NO_2+NO_3+2*(N_2O_5)+HNO_3+HO_2NO_2+ClONO_2+BrONO_2$), reactive hydrogen

262 ($HO_x = OH+HO_2$), and temperature (T). Each term on the right hand side of the equation

263 (1) then gives the "contribution" of the response in ozone due to a change in X, and the

264 role the corresponding mechanism plays in the ozone evolution (i.e., $m_{EESC}\Delta EESC$ is the

265 contribution due to changes in EESC, and the role of changes in halogen ozone-loss

266 cycles). We chose HO_x as an explanatory variable rather then H_2O even though it is a

267 shorter lived species to address feedbacks which are discussed in section 6 which would

268 not be seen using H_2O.

269 Rather than using the above four quantities as explanatory variables X in the

270 MLR analysis, an alternative approach would be to use the surface concentrations of the

271 ODSs and GHGs as the independent variables X. *Stolarski et al.* [2009] used this

272 approach when examining temperature changes in the GEOS CCM simulations

273 considered here. Also, *Shepherd and Jonsson* [2008] used ODSs and CO_2 to separate

274 their impact on temperature and ozone changes but could not quantify the impact of other

275 GHGs, although they are likely to have a smaller impact. However, as discussed above,

276 changes in HO_x and NO_y do not simply follow changes in CH_4 and N_2O, respectively,

277 and regressing against CH_4 and N_2O will not necessarily isolate the role of changes in the

278 hydrogen and nitrogen cycles in the response of ozone. Furthermore, the time series of

279 CO_2 and N_2O are not independent in terms of correlation for either scenario, and neither

280 are CO_2 and CH_4 for the A2 scenario (see Figure 1). This means that the MLR could not

281 separate the impact of these fields.

282   The model output used in the MLR analysis is from instantaneous output from the

283 1st day of each month since not all variables were saved as monthly averages, however

284 using monthly mean data should not materially affect the results. This analysis was done

285 for individual months as well as annual averages. Here, we focus on presenting results

286 calculated using annual averages. Thus we examine interannual and longer timescale

287 variations in ozone. The above MLR analysis presented below uses all 140 years of the

288 GEOS CCM simulations to determine the coefficients m_X. Calculations using shorter

289 time periods (i.e. different start or end dates) show some sensitivity to the period used

290 (e.g., if the start date is between 1960 and 1990 and the end date between 2050 and 2100

291 there is some variation in the coefficients).

292   There are several complications with the above linear regression approach. First,

293 other mechanisms that are not considered in the regression (e.g., transport) could play a

294 role. Second, significant correlations can exist between the temporal variations of the

295 quantities, i.e., the quantities are not necessarily independent. Third, a high correlation

296 between ozone and a quantity does not show causality, as ozone could be causing the

297 quantity to change, or changes in another quantity could be causing both ozone and the

298   quantity of interest to change in a correlated way. Temperature and ozone in the upper

299   stratosphere is an example of this third complication: Changes in ozone cause, through

300   changes in short-wave heating, changes in temperature. At the same time, changes in

301   temperature cause, through changes in reaction rates, differences in the response of

302   ozone. Also, the relationship between the variables we use and ozone may not be linear.

303   Because of the above complications caution must be applied when interpreting the MLR

304   results presented below. Additional discussion and analysis of these issues is included

305   below.

306

307

308   ## 5 Relative Contributions to Ozone Changes

309

310   We now use the MLR analysis described in Section 4 to quantify the role of

311   different mechanisms in causing the ozone changes in the A1b and A2 simulations. We

312   first examine the ozone evolution in the tropical upper stratosphere. As discussed above,

313   the simulated upper stratospheric ozone in the 2090s is greater than in the 1960s.

314   Examples are shown in Figures 3a and 3b, where the simulated evolution of annually

315   averaged ozone over 10°S-10°N, at 2.9 hPa for the A1b and A2 simulations, respectively,

316   are shown (black curves). This shows that the ozone decreases rapidly from 1960 to

317   2000, and then increases, at roughly the same rate, back to 1960s values by the 2030s.

318   The ozone continues to increase, although at a slower rate, and by the end of the century

319   the ozone is significantly higher ($\approx$ 20%) than in the 1960s.

320   From the MLR analysis it is possible to estimate the contribution of different

321 mechanisms to the changes in ozone. Specifically, the coefficients m_X from equation (1)

322 are multiplied by the simulated change in each quantity ΔX to determine the contribution

323 to the change in ozone (i.e. $m_{EESC}\Delta EESC$ is the contribution due to changes in EESC).

324 The individual "contributions" for each quantity are shown in Figure 3c for A1b and

325 Figure 3d for A2, and the ozone calculated from the sum of these contributions added to

326 the mean ozone value (dotted black curves) are shown as the magenta curves in Figures

327 3a and 3b. There is excellent agreement between this "reconstruction" and the simulated

328 ozone change. In the A1b simulation the long-term evolution of ozone at 2.9 hPa is

329 dominated by changes in EESC (red curve) and T (blue curve), with negligible

330 contributions from variations in NO_y (orange curve) and HO_x (green curve), see Figure

331 3c. The situation is somewhat different for the A2 scenario, where there is a larger trend

332 in T, NO_y, and HO_x at this level and changes in NO_y and HO_x now contribute to the

333 ozone change. However, the decrease in O_3 due to the increase in NO_y and HO_x is

334 canceled out by the larger increase due to the larger T trend, and the net O_3 change in A2

335 is similar to that of A1b.

336 Figures 3a and 3b show that the ozone reconstruction from the MLR analysis

337 using T, EESC, NO_y, and HO_x reproduces the simulated ozone evolution in the tropics at

338 2.9 hPa. However, this good agreement may not apply throughout the stratosphere. To

339 assess how well the model ozone variability is explained by the MLR analysis the square

340 of the correlation coefficient between the MLR reconstruction and simulated ozone is

341 shown in Figure 4, for (a) the original time series, and (b) a filtered time series with low

342 frequency variability removed. Since significant autocorrelation exists over many

343 locations in the original time series we focus on the time series in Figure 4b which does

344   not have significant autocorrelations. Figure 4b shows that the fit between the MLR

345   analysis and simulated ozone is very good in the extra-polar upper stratosphere (e.g., in

346   the tropical upper stratosphere over 90% of the interannual variability is explained by the

347   MLR analysis), but the fit is a lot poorer in polar regions and in the middle and lower

348   stratosphere.   This poorer fit is most likely due to the larger role of transport, which is

349   not explicitly accounted for in the MLR analysis. Because of the above we focus our

350   MLR analysis on ozone changes in the extra-polar upper stratosphere.

351   The analysis at 2.9 hPa indicates that changes in NO_y and HO_x make negligible

352   contributions to ozone changes for the A1b simulation, but NO_y and HO_x do make

353   significant contributions for the A2 simulation. However, the contributions of the

354   different quantities vary with altitude. This is illustrated in Figures 3e-h which shows the

355   contributions for 0.9 hPa and 5.6 hPa. (The simulated ozone and MLR reconstruction are

356   not shown as the evolution and agreement is similar to that for 2.9 hPa.) At 0.9 hPa

357   (Figures 3e,f) HO_x related ozone loss is more important than at 2.9 hPa. This is

358   especially evident in the A2 scenario (Figure 3f) where there is a much larger CH_4 trend

359   yielding a larger HO_x trend. The larger HO_x related ozone loss is again offset by larger T

360   contributions. In contrast to 0.9 hPa, NO_y related ozone loss is important at 5.6 hPa for

361   the A2 scenario (Figures 3h). In the A1b simulation NO_y variations contribute to year to

362   year variability but not to the long term trend (Figure 3g), whereas in the A2 simulation

363   variations in NO_y contribute to the long-term behavior (Figure 3h). The trend due to

364   increased NO_y results in an ozone decrease of 0.5 ppm from the 1960s to the 2090s. As

365   with the larger changes in T and HO_x at 0.9 hPa, the larger changes in T and NO_y in the

366   A2 simulation at 5.6 hPa cause larger changes in ozone, but these changes are of opposite

367   sign and the net change in ozone in A2 is similar to that in the A1b simulation.

368   Close inspection of Figures 3c-h shows the relative contributions of the different

369   mechanisms to changes in ozone vary with time. This is quantified in Figure 5 which

370   shows the vertical variation of the changes in tropical ozone and individual contributions

371   of different mechanisms for the A1b (solid curves) and A2 (dashed curves) simulations,

372   over (a) 1960-2000, (b) 2000-2100, and (c) 1960-2100.

373   Over the 1960 to 2000 period both simulation have identical forcings and only

374   vary by the initial conditions, so very similar changes occur in each simulation. The

375   largest change in ozone (-0.6 ppm) occurs in the upper stratosphere at about 3 hPa. This

376   change is mostly caused by the increasing levels of EESC (-1.1 ppm) and is somewhat

377   offset by the decreasing temperature (0.5 ppm). The cooling of the upper stratosphere is

378   mostly due to increases in GHGs like CO_2 but also due to decreased ozone (see Section

379   6). Over the last forty years, NO_y and HO_x increases make an insignificant contribution

380   to ozone changes in the upper stratosphere. The ozone changes in the lower stratosphere

381   are much smaller than in the upper stratosphere, and are discussed briefly below.

382   The ozone change over the 21st century (2000s to 2090s) is very different than

383   from 1960 to 2000: Upper stratospheric ozone increases over this period due to decreases

384   in EESC and decreases in T (Figure 5b). There are very similar ozone evolutions for the

385   two different scenarios, but the contributions from the different mechanisms vary. As

386   discussed above, there is a larger positive increase in upper stratospheric ozone due to

387   temperature changes in A2 than in A1 due to larger temperature decreases in A2. These

388   increases are almost entirely balanced by increased loss from NO_y and HO_x increases,

389   with losses due to NO_y largest between 10 and 3 hPa and those due to HO_x largest above

390   5 hPa (consistent with results of *Portmann and Solomon*, 2007), resulting in very similar

391   ozone evolutions.

392   Figure 6a shows that the m_X calculated from the two simulations are very similar,

393   implying that the differences in contributions in the two simulations are due to

394   differences in the temperature and composition (Figure 6b) rather than differences in the

395   sensitivities. The 3σ confidence intervals of the sensitivities are also shown in Figure 6a

396   (thin curves), and these indicate that uncertainties with this analysis are generally largest

397   in the lower portions of the stratosphere while in the upper portions, the confidence

398   intervals are much smaller with, the largest are associated with the calculated NO_y

399   sensitivities. The cooling with respect to 2000s values in A2 is significantly larger (2 to 4

400   K, see Figure 6b), causing a larger increase in middle and upper stratospheric ozone. The

401   differences in NO_y and HO_x are also larger in the A2 simulation (Figure 6b), consistent

402   with the increased levels of N_2O and CH_4 respectively, shown in Figure 1a. As discussed

403   above the increases in NO_y and HO_x are not necessarily the same as those in N_2O and

404   CH_4. For example, the increase in middle-upper stratospheric NO_y is much smaller than

405   the increase in tropospheric N_2O, due to cooling in the middle and upper stratosphere,

406   which increases NO_y loss [*Rosenfield and Douglass*, 1998]. Also, the NO_y-related ozone

407   loss rates are only weakly dependent on T [e.g., *Jonsson et al.*, 2004], so the temperature

408   decrease does not cause a significant difference in this loss.

409   The changes over the complete period of the simulations (1960s to 2090s) are

410   shown in Figure 5c. These are similar to the 21st century change (Figure 5b), except there

411   is only a small contribution for EESC over the complete period, and ozone changes are

412   dominated by the T changes.

413   Although we focus here on upper stratospheric ozone changes, we briefly

414   comment on the decrease in tropical lower stratospheric ozone (Figure 5). Although the

415   MLR analysis attributed most of this decrease to changes in T, the ozone responses are

416   primarily due increases in tropical upwelling. An increase in tropical upwelling in the

417   lower stratosphere will, if no other changes, result in a decrease in ozone. Furthermore,

418   increases in the upwelling and decreases in ozone will both lead to a decrease in

419   temperature (through adiabatic cooling and reduced heating, respectively), and hence

420   produce correlated changes in ozone and temperature. The larger upwelling increases and

421   tropical lower stratospheric ozone decreases in A2 are consistent with larger increases in

422   SSTs within the A2 simulation, see *Oman et al.* [2009]. The relationship between

423   upwelling and decreases in tropical lower stratospheric ozone concentrations have been

424   the focus of some recent studies including *Lamarque et al.* [2008] and *Li et al.* [2009].

425   The ozone changes and contributions from relative mechanisms for middle

426   latitudes are similar to that for the tropical stratosphere, e.g., compare Figures 7 and

427   Figure 5. In the midlatitudes of both hemispheres (30-50° N and S) there is a decrease in

428   upper stratospheric ozone from the 1960s to 1990s due to increases in EESC (with a

429   small compensating increase due to cooling), while the upper stratospheric ozone is

430   projected to increase over the 21st century due to increases in EESC and further cooling

431   (Figure 7). As in the tropics, the larger ozone increase in the A2 simulation is due to

432   larger cooling, which is canceled by larger ozone losses related to larger changes in NO_y

433   and HO_x in the A2 simulation.

434

435

6 Fixed Halogen Simulation

436

437

438   Two questions that arise when using the MLR analysis are: how representative are

439   the calculated sensitivities (i.e. can they be applied to other simulations) and can the

440   MLR represent some of the feedbacks that occur in the climate system (i.e. separating the

441   effect of CO_2 on T from that due to O_3 loss from EESC. To examine these issues we use

442   an additional GEOS CCM simulation with the same SSTs and GHGs as the A1b

443   simulation, but with halogens fixed at 1960 levels. As discussed in *Waugh et al.* [2009],

444   the difference in ozone between the A1b and "fixed-halogen" simulations is the change in

445   ozone due to EESC, with this EESC-induced change including both the direct EESC

446   chemical impact and any 'indirect' feedbacks.

447   We first test whether the regression coefficients (sensitivities) m_X calculated

448   above can be used to reconstruct the ozone in the fixed-halogen simulation. As above,

449   we multiply the coefficients by the change in each quantity (e.g., EESC, T, NO_y, HO_x) to

450   determine the individual contributions to the ozone change, and then compare the sum of

451   these contributions with the simulated ozone change. Figure 8a shows the evolution of

452   tropical upper stratospheric (10°S-10°N at 2.9 hPa) ozone from the A1b and fixed-

453   halogen simulations, together with the reconstructed ozone (using the coefficients m_X

454   calculated from the A1b simulation for both reconstructions). There is good agreement

455   between the simulated and reconstructed ozone for the fixed-halogen simulation, showing

456   that the coefficients calculated here can be applied to different simulations.

457   We now examine the direct and indirect EESC impact on ozone. Waugh et al.

458   (2009) discussed the difference in ozone between the A1b and "fixed-halogen"

459   simulations. This net change in ozone is due to EESC, with this EESC-induced change

460   including both the direct EESC chemical impact and any 'indirect' feedbacks. Equation

461   (1) can also be used to separate different effects if the difference between the A1b and

462   fixed-halogen simulation is used for ΔX. This is opposed to using the temporal change in

463   a single simulation (ΔT = difference in T due to changes in EESC, so that $m_T \Delta T$ reflects

464   the change in O_3 due to T feedback). Figure 8b compares the difference in O_3 at 2.9 hPa

465   between the A1b and fixed-halogen simulation with the contributions due to differences

466   in EESC, T, NO_y, and HO_x, as well the sum of these contributions. There is again good

467   agreement between the actual and reconstructed O_3 (solid and dashed black curves nearly

468   overlain). The direct impact of EESC changes (red curve) dominates the change in O_3.

469   The blue curve represents, the negative feedback due to temperature change from the

470   direct O_3 loss caused by EESC, and it is significant. For example, in 2000 there is a total

471   O_3 loss of around 1.0 ppm which is a balance between a 1.2 ppm loss due to EESC

472   chemical loss and a 0.2 ppm increase due to the cooling associated with this O_3 loss.

473   At 0.9 hPa there is not only a negative feedback from cooler temperatures, but

474   also a negative feedback from HO_x (Figure 8c). This occurs as Cl and HCl destroy HO_x to

475   form H_2O and O_2 [*Brasseur et al.*, 1999].

476

477                    $$Cl + HO_2 \rightarrow HCl + O_2$$

478                    $$\underline{OH + HCl \rightarrow Cl + H_2O}$$

479   Net: $$OH + HO_2 \rightarrow H_2O + O_2$$
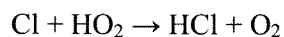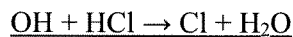
480

481

482 As a result of the temperature and HO_x feedback the net ozone loss at 0.9 hPa is around

483 50% less than that expected from destruction due to EESC. Much smaller feedbacks are

484 calculated at 5.6 hPa, and the direct loss due to EESC is very close to the modeled ozone

485 loss (Figure 8d).

486

487 ## 6.1 Chemical Box Model Analysis

488

489 As a further test of the robustness of the above MLR results we compare the

490 coefficients m_X obtained from the MLR analysis with the sensitivities obtained from

491 chemical box model calculations [*Kawa et al.*, 1997]. In the upper stratosphere, ozone is

492 close to photochemical steady state, and chemical box model calculations can be used to

493 estimate the sensitivity of ozone to the changes in different inputs.

494 To estimate the ozone sensitivities a reference box model calculation is first

495 performed using the mixing ratios of chemical species, overhead ozone, and temperature

496 for a particular location and time from the GEOS CCM simulation using the A1b

497 scenario. In this case we used an average 1960-2100 value to represent what was

498 calculated in the MLR analysis. Then a series of perturbation calculations is performed,

499 where a single quantity (e.g. temperature) is increased and decreased from its reference

500 value. For EESC, Cly was perturbed ± 0.1 ppb and Bry perturbed ± 1 ppt; temperature

501 was perturbed ± 5K; and NOy was perturbed ± 1 ppb. Each simulation was run for 20

502 days, by which time the solution has closely approached steady state. The resulting

503 change in ozone gives an estimate of the sensitivity of ozone to changes in this quantity,

504 e.g. $\Delta O_3 / \Delta X$ provides an estimate of sensitivity of ozone to changes in variable X. This

505   sensitivity can then be directly compared with the coefficients m_x from equation (1).

506   Figure 6a shows the variation in calculated steady-state ozone to changes in T,

507   EESC, and NO_y (colored X's) for reference calculations based on simulated fields at

508   several levels between 6.9 and 0.9 hPa for July at 2°N. Although we use annual average

509   values for the MLR analysis, tests using other months in the chemical box model

510   produced only small changes. These values are generally in very good agreement with the

511   coefficients from the MLR analysis. Some disagreement is seen at 5.6 and 6.9 hPa with

512   slightly higher EESC, NO_y, T sensitivities from the chemical box. NO_y sensitivities are in

513   general slightly larger in the box model than calculated in the MLR analysis. It is not

514   clear at this point why there are some differences seen in the sensitivities between the

515   MLR analysis and the box model. Even though there is some disagreement, overall the 2

516   methods show a similar picture and give us confidence in the MLR-based attribution of

517   the relative contributions of different factors to the changes in ozone.

518

519   **7 Conclusions**

520

521   In this study we have quantified the contribution of different mechanisms to

522   changes in upper stratospheric ozone from 1960 to 2100 in GEOS CCM simulations, and

523   separated the direct and indirect impacts of EESC on ozone. Simulations using two

524   different GHG scenarios (A1b and A2 from *IPCC* 2001) were considered, and even

525   though there are significant differences in the GHG concentrations in the latter half of the

526   21st century, there is a very similar increase in upper stratospheric ozone over the 21st

527   century. Isolation of different mechanisms using multiple linear regression (MLR) shows

528   that the similar ozone evolution is because of compensating effects of different

529   mechanisms.   In the A1b scenario the increase in ozone is caused by decreases in

530   halogenated ozone-depleting substances and cooling, which is largely due to increased

531   greenhouse gases, which alters the kinetics rate of ozone destruction, with the two

532   mechanisms making roughly equal contributions to the ozone change. Changes in

533   abundance of reactive nitrogen and hydrogen play only a minor role in long-term changes

534   in the A1b scenario. In contrast, in the A2 simulation there are significant increases in

535   NO_y and HO_x that cause a long-term negative decrease in ozone. These decreases are

536   largely offset by a larger positive contribution from cooler temperatures, and the ozone

537   evolution in A2 ends up being very similar to that in A1b.

538   The MLR analysis, together with a fixed halogen simulation, was also used to

539   separate the direct chemical impact and indirect feedbacks of EESC on ozone. The

540   indirect impact and mechanisms were shown to vary with altitude. At 5.6 hPa the indirect

541   impacts are small, but make significant contributions at 2.9 and 0.9 hPa. At 2.9 hPa there

542   is a negative feedback due to temperature increases from the direct O_3 loss due to EESC

543   chemistry. This feedback is around 15% the direct EESC impact. At 0.9 hPa there are

544   negative feedbacks from temperature and from changes in HO_x due to changes in EESC,

545   and the sum of these are around 50% the direct EESC impact.

546   The results presented above are based on simulations from a single model, and it

547   will be important to consider simulations from other models. Preliminary application of

548   MLR method to A1b simulations from several of the CCMs examined in *Eyring et al.*

549   [2007] yields very similar results to those presented here for the GEOS CCM (not

550   shown).   In particular, the sensitivities are very similar, and differences in ozone

551 evolution can be related to differences in simulated EESC, T, and NO_y fields. As well as

552 considering other models it will be important to consider a wider range of GHG

553 scenarios. The very similar ozone evolution for the A1B and A2 GHG scenarios

554 considered here might lead one to think that the ozone evolution would be similar for all

555 likely GHG scenarios. However, the similarity between the A1B and A2 scenarios

556 considered here occurs by the chance cancellation of differences in temperature and

557 nitrogen and hydrogen loss cycles, and this is unlikely to be the case for all possible

558 scenarios (e.g., for the A1F1 and B1 scenarios). It will therefore be important to perform

559 simulations with a wider range of GHG scenarios when making projections of

560 stratospheric ozone.

561 This analysis of models using MLR raises the possibility of using MLR analysis

562 to separate the contributions of changes in EESC and T to observed ozone changes. One

563 difficulty with applying this method to data is the availability of simultaneous time series

564 of observed ozone, EESC, T and other quantities used in the MLR analysis. Another

565 issue is the need to consider time periods over which the different quantities have

566 sufficiently different temporal variations to be isolated in the MLR analysis. For the 140

567 years of simulation considered here this is possible for EESC and T, but this may not be

568 the case for shorter periods and more analysis is need to determine over which period

569 data will be required to perform this analysis.

570

571

572

573   **8 Acknowledgments**

9 References

Austin, J., and R. J. Wilson (2006), Ensemble simulations of the decline and recovery of stratospheric ozone. *J. of Geophys. Res.*, 111, D16314, doi:10.1029/2005JD006907.

Basseur, G. and M. H. Hitchman (1988), Stratospheric Response to Trace Gas Perturbations: Changes in Ozone and Temperature Distributions. *Science*, 240, 634-367.

Brasseur, G. P., J. J. Orlando, and G. S. Tyndall (1999), Atmospheric Chemistry and Global Change. Oxford University Press, Oxford.

Chipperfield, M. P., and W. Feng (2003), Comment on: "Stratospheric Ozone Depletion at northern mid-latitudes in the 21st century: The importance of future concentrations of greenhouse gases nitrous oxide and methane", *Geophys. Res. Lett.*, *30*, 1389, doi: 10.1029/2002GL016353.

Daniel, J. S., S. Solomon, R. W. Portmann, R. R. Garcia (1999), Stratospheric ozone destruction: The importance of bromine relative to chlorine. *J. Geophys. Res.*, 104, 23,871-23,880.

Eyring, V., and Coauthors (2006), Assessment of temperature, trace species, and ozone in chemistry-climate model simulations of the recent past. *J. Geophys. Res.*, 111, D22308, doi:10.1029/ 2006JD007327.

Eyring, V., and Coauthors (2007), Multimodel projections of stratospheric ozone in the 21st century, J. Geophys. Res., 112, D16303, doi:10.1029/ 2006JD008332.

Haigh, J. D. and J. A. Pyle (1979), A two-dimensional calculation including atmospheric carbon dioxide and stratospheric ozone, *Nature*, 279, 222-224.

606   IPCC (2001), Third Assessment Report, Working Group I, Intergovernmental Panel on

607   Climate Change, 2001.

608   Jonsson, A. I., et al. (2004), Doubled CO_2 -induced cooling in the middle atmosphere:

609   Photochemical analysis of the ozone radiative feedback, *J. Geophys. Res.*, 109,

610   D24103, doi:10.1029/ 2004JD005093.

611   Kawa, S.R., et al. (1997), Activation of chlorine in sulfate as inferred from aircraft

612   observations, *J. Geophys. Res.*, 102, 3921-3933.

613   Kawa, S. R., R. Bevilacqua, J. J. Margitan, A. R. Douglass, M. R. Schoeberl, K. Hoppel,

614   and B. Sen (2002), The interaction between dynamics and chemistry of ozone in the

615   set-up phase of the northern hemisphere polar vortex, *J. Geophys. Res.*, 107, 8310,

616   doi: 10.1029/2001JD001527.

617   Lamarque, J.F, and S. Solomon (2008), Identifying the role of vertical velocity trends in

618   explaining tropical in lower stratospheric ozone trends, *J. Geophys. Res.*, submitted.

619   Li, F., R.S. Stolarski, and P.A. Newman (2009), Stratospheric ozone in the post-CFC era,

620   *Atmos. Chem. Phys.*, 9, 2207-2213.

621   Newchurch, M. J., E.-S. Yang, D. M. Cunnold, G. C. Reinsel, J. M. Zawodny, and J. M.

622   Russell III (2003), Evidence for slowdown in stratospheric ozone loss: First stage of

623   ozone recovery, *J. Geophys. Res.*, 108, D16, 4507, doi:10.1029/2003JD003471.

624   Oman, L., D. W. Waugh, S. Pawson , R. S. Stolarski, J. E. Nielsen (2008), Understanding

625   the Changes of Stratospheric Water Vapor in Coupled Chemistry-Climate Model

626   Simulations. *J. Atmos. Sci.*, *65*, doi:10.1175/2008JAS2696.1.

627   Oman, L., D. W. Waugh, S. Pawson, R. S. Stolarski, and P. A. Newman (2009), On the

628   influence of anthropogenic forcings on changes in the stratospheric mean age, *J.*

629 *Geophys. Res.*, 114, D03105, doi:10.1029/2008JD010378.

630 Pawson S., R. S. Stolarski, A. R. Douglass, P. A. Newman, J. E. Nielsen, S. M. Frith, and

631 M. L. Gupta (2008), Goddard Earth Observing System chemistry-climate model

632 simulations of stratospheric ozone-temperature coupling between 1950 and 2005, *J.*

633 *Geophys. Res.,* 113, D12103, doi:10.1029/2007JD009511.

634 Portmann R.W. and S. Solomon (2007), Indirect radiative forcing of the ozone layer

635 during the 21st century, *Geophys Res. Lett.,* 34, L02813, doi:10.1029/2006GL028252.

636 Randeniya, L. K., P. F. Vohralik, and I. C. Plumb (2002), Stratospheric ozone depletion

637 at northern mid latitudes in the 21st century: The importance of future concentrations

638 of greenhouse gases nitrous oxide and methane, *Geophys. Res. Lett.,* 29 (4), 1051,

639 doi: 10.1029/2001GL014295

640 Rayner, N. A., D. E. Parker, E. B. Horton, C. K. Folland, L. V. Alexander, D. P. Rowell,

641 E. C. Kent, and A. Kaplan (2003), Global analyses of sea surface temperature, sea

642 ice, and night marine air temperature since the late nineteenth century, *J. Geophys.*

643 *Res.*, 108(D14), 4407, doi:10.1029/2002JD002670.

644 Rosenfield, J.E., and A.R. Douglass (1998), Doubled CO_2 effects on NO_y in a coupled

645 2-D model, *Geophys. Res. Lett.* 25, 4381-4384.

646 Rosenfield, J. E., A. R. Douglass, and D. B. Considine (2002), The impact of increasing

647 carbon dioxide on ozone recovery, *J. Geophys. Res.*, 107 (D6), 4049, doi:

648 10.1029/2001JD000824.

649 Shindell, D. T., D. Rind and P. Lonergan (1998), Climate Change and the Middle

650 Atmosphere. Part IV: Ozone Response to Doubled CO_2. *J. Clim, 11,* 895-918.

651 Shepherd, T. G. (2008), Dynamics, Stratospheric Ozone, and Climate Change. *Atmos.*

652   *Ocean*, 46, 117-138.

653   Shepherd, T. G., and A. I. Jonsson (2008), On the attribution of stratospheric ozone and

654   temperature changes to changes in ozone-depleting substances and well-mixed

655   greenhouse gases, *Atmos. Chem. Phys.*, 8, 1435-1444.

656   Stolarski, R. S., et al. (2006), An ozone increase in the Antarctic summer stratosphere: A

657   dynamical response to the ozone hole, *Geophys. Res. Lett.* 33, L21805,

658   doi:10.1029/2006GL026820.

659   Stolarski, R. S., A. R. Douglass, P. A. Newman, S. Pawson, and M. R. Schoeberl (2009),

660   Relative contribution of greenhouse gases and ozone-depleting substances to

661   temperature trends in the stratosphere: a chemistry/climate model study, Submitted to

662   *J. Clim.*

663   Waugh, D. W., L. Oman, S. R. Kawa, R. S. Stolarski, S. Pawson, A. R. Douglass, P. A.

664   Newman, and J. E. Nielsen (2008), Impact of climate change on stratospheric ozone

665   recovery, submitted to *Geophys. Res. Lett.*

666   World Meteorological Organization (WMO)/United Nations Environment Programme

667   (UNEP) (2003), Scientific Assessment of Ozone Depletion: 2002, World

668   Meteorological Organization, Global Ozone Research and Monitoring Project, Report

669   No. 47, Geneva, Switzerland.

670   World Meteorological Organization (WMO)/United Nations Environment Programme

671   (UNEP) (2007), Scientific Assessment of Ozone Depletion: 2006, World

672   Meteorological Organization, Global Ozone Research and Monitoring Project, Report

673   No. 50, Geneva, Switzerland.

674

675

676   **10 Figure Captions**

677

678   Figure 1. Temporal Variation of (a) surface GHGs (solid – A1b and dashed – A2) and

679   halogens and (b) total or partial column ozone averaged between 60°S and 60°N,

680   between 1960 and 2100 (solid – A1b and dashed – A2).

681

682   Figure 2. Difference in ozone (ppm) between 1960s to 2090s (2090s-1960s) for (a)

683   annual for A1b scenario, (b) annual for A2 scenario. Also, for same time period changes

684   in (c) EESC (ppb) for A1b, (d) EESC (ppb) for A2, (e) Temperature (K) for A1b, (f)

685   Temperature (K) for A2.

686

687   Figure 2 (cont.). Difference in annual NO_y (ppb) between 1960s to 2090s (2090s-1960s)

688   for (g) A1b scenario, (h) A2 scenario, (i) HO_x (ppt) for A1b, and (j) HO_x (ppt) for A2, (k)

689      $\overline{w}^*$ (mm/s) for A1b, (l) $\overline{w}^*$ (mm/s) for A2.

690

691   Figure 3. Evolution of annual average ozone at (a) 2.9 hPa, for A1b and (b) 2.9 hPa, for

692   A2, 10°S-10°N. Also shown is the contribution of different mechanisms for (c,d) 2.9 hPa,

693   (e,f) 0.9 hPa, and (g,h) 5.6 hPa for each scenario.

694

695   Figure 4. Annual correlation coefficient squared for the (a) original model ozone time

696   series and MLR fit and, (b) a filtered time series with low frequency variability removed

697   by applying a 1:2:1 filter iteratively 30 times to each quantity.

698

699   Figure 5. Vertical variation of changes in ozone (solid black curve) and individual

700   contribution of different mechanisms for annual averages over the tropics. The changes

701   are for (a) 1990s-1960s P1 (solid curve) and P2 (dashed curve), (b) 2090s-2000s A1b

702   (solid curve) for A2 (dashed curve) scenario, 2090s-1960s A1b (solid curve) for A2

703   (dashed curve) scenario.

704

705   Figure 6. Sensitivities (a) of ozone to various factors (thick curves) and 3σ confidence

706   intervals (thin curves) for annual averages over the tropics ($10°$S-$10°$N) with the

707   overplotted X's showing the chemical box model calculations and the 2090s-2000s

708   change (b) in T, EESC, and NO_y, and HO_x divided by 100, and the contribution for A1b

709   (solid curves) and A2 (dashed curves).

710

711   Figure 7. Vertical variation of changes in ozone (solid black curves) and individual

712   contribution of different mechanisms for annual averages over (a,c) 50-$30°$S and (b,d) 30-

713    $50°$N. The changes are for (a,b) 1990s-1960s P1 (solid curves) and P2 (dashed curves),

714   and (c,d) 2090s-2000s A1b (solid curves) for A2 (dashed curves) scenario.

715

716   Figure 8. Evolution of ozone and from MLR for (a) 2.9 hPa, $10°$S-$10°$N for A1b

717   simulation and for a fixed-halogen (Low Cl) simulation (upper curve, with the fit from

718   A1b MLR sensitivities). Difference in ozone between the A1b and fixed-halogen

719   simulation (solid black curve), and contributions due to EESC (red curve), T (blue), NO_y

720   (orange), and HO_x (green) as well as the sum of these contributions (dashed black curve)

721   for (b) 2.9 hPa, $10°$S-$10°$N. Also shown are the individual contributions at (c) 0.9 hPa

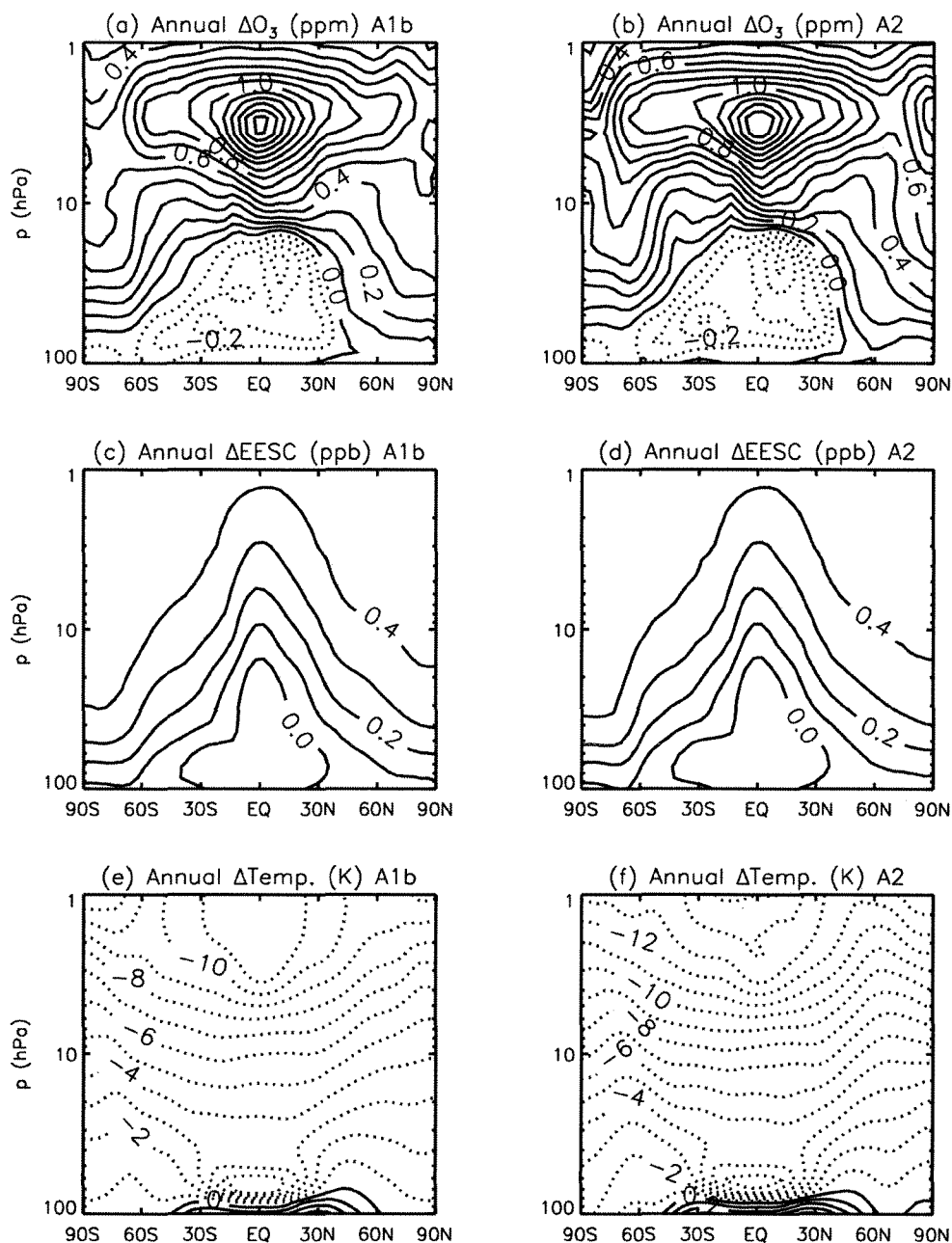722   (note the different scale) and (d) 5.6 hPa.

723
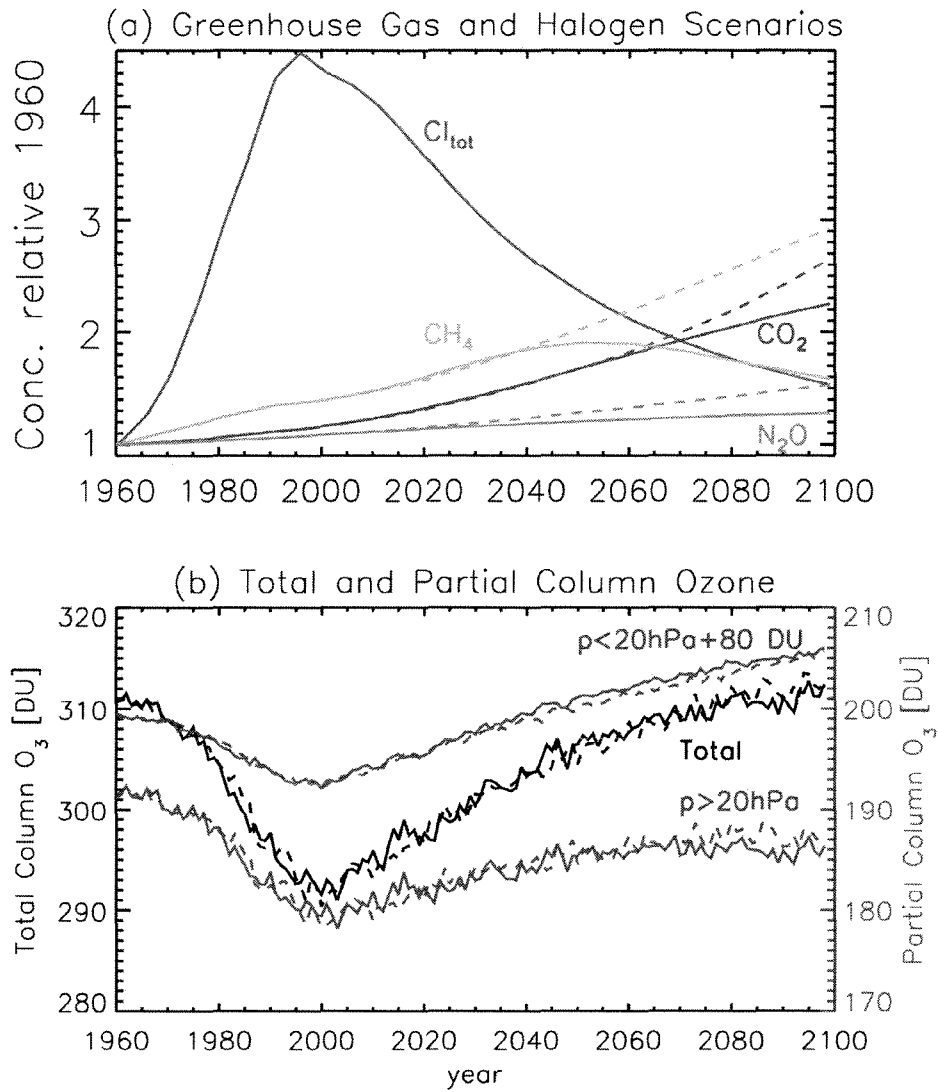
Figure 1. Temporal Variation of (a) surface GHGs (solid – A1b and dashed – A2) and halogens and (b) total or partial column ozone averaged between 60°S and 60°N, between 1960 and 2100 (solid – A1b and dashed – A2).

729
730 Figure 2. Difference in ozone (ppm) between 1960s to 2090s (2090s-1960s) for (a)
731 annual for A1b scenario, (b) annual for A2 scenario. Also, for same time period changes
732 in (c) EESC (ppb) for A1b, (d) EESC (ppb) for A2, (e) Temperature (K) for A1b, (f)
733 Temperature (K) for A2.
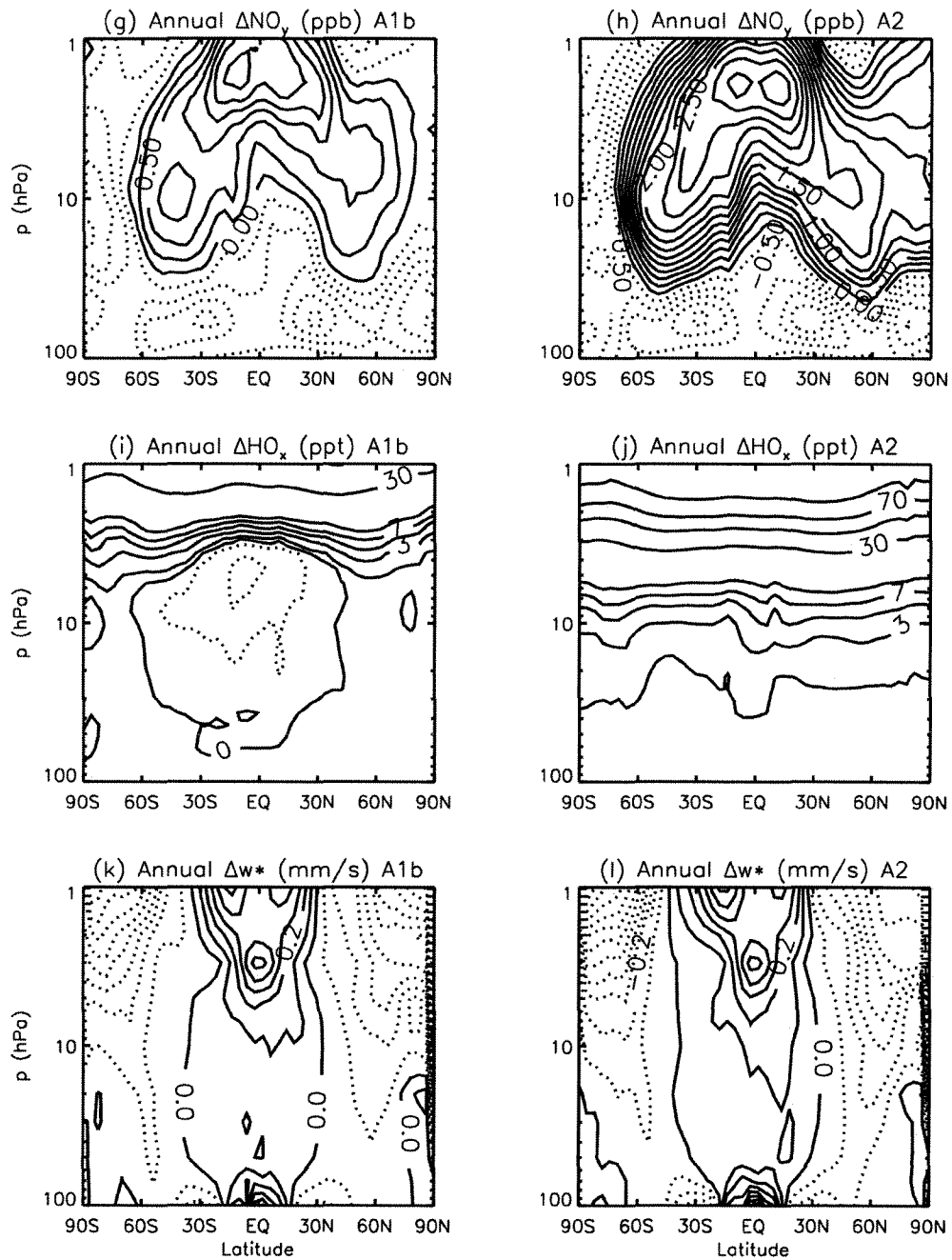
734
735
736   Figure 2 (cont.). Difference in annual NO_y (ppb) between 1960s to 2090s (2090s-1960s)
737   for (g) A1b scenario, (h) A2 scenario, (i) HO_x (ppt) for A1b, and (j) HO_x (ppt) for A2, (k)
738    $\overline{w}^*$ (mm/s) for A1b, (l) $\overline{w}^*$ (mm/s) for A2.
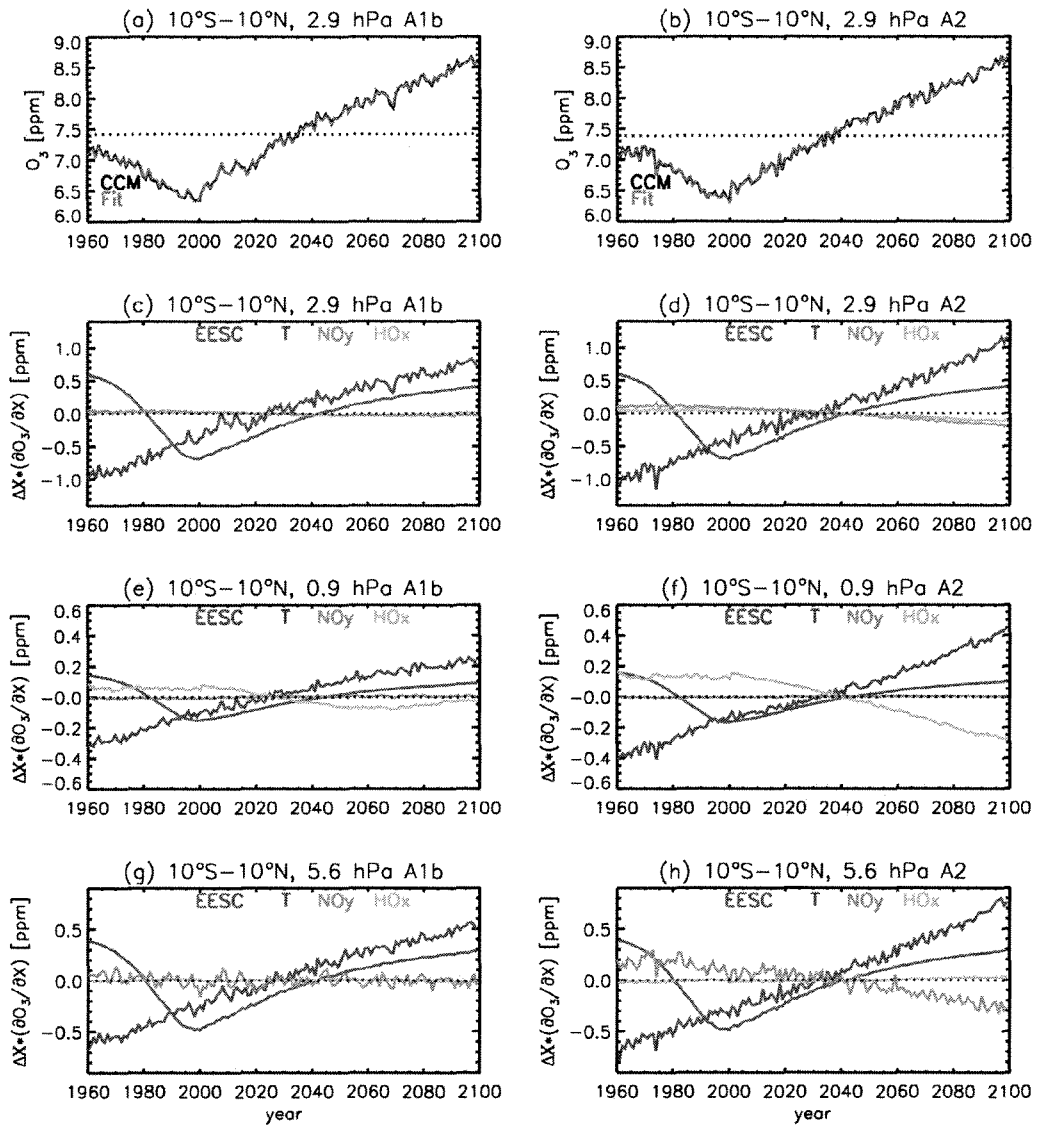
739
740 Figure 3. Evolution of annual average ozone at (a) 2.9 hPa, for A1b and (b) 2.9 hPa, for
741 A2, 10°S-10°N. Also shown is the contribution of different mechanisms for (c,d) 2.9 hPa,
742 (e,f) 0.9 hPa, and (g,h) 5.6 hPa for each scenario.
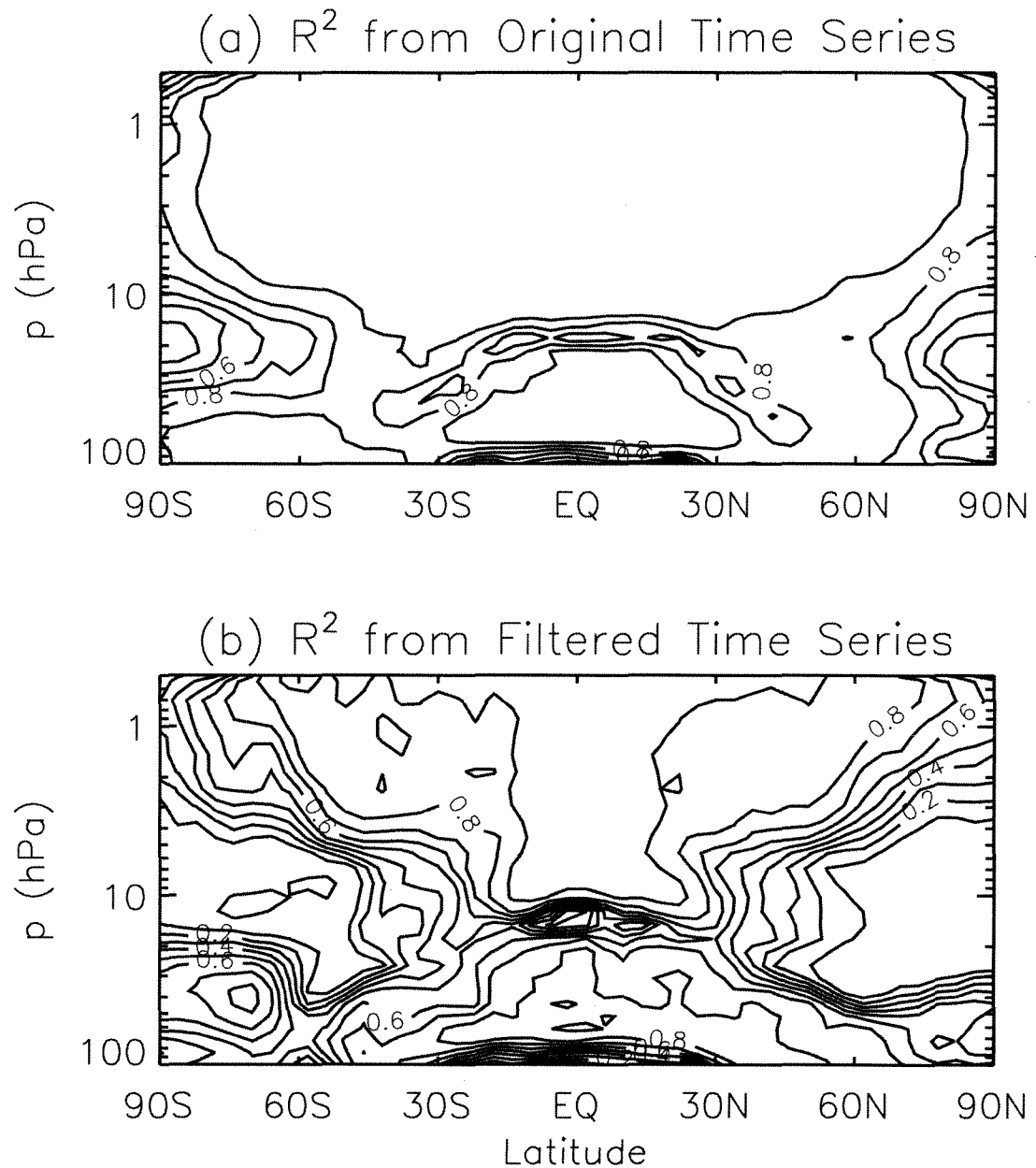
743
744　Figure 4.　Annual correlation coefficient squared for the (a) original model ozone time
745　series and MLR fit and, (b) a filtered time series with low frequency variability removed
746　by applying a 1:2:1 filter iteratively 30 times to each quantity.
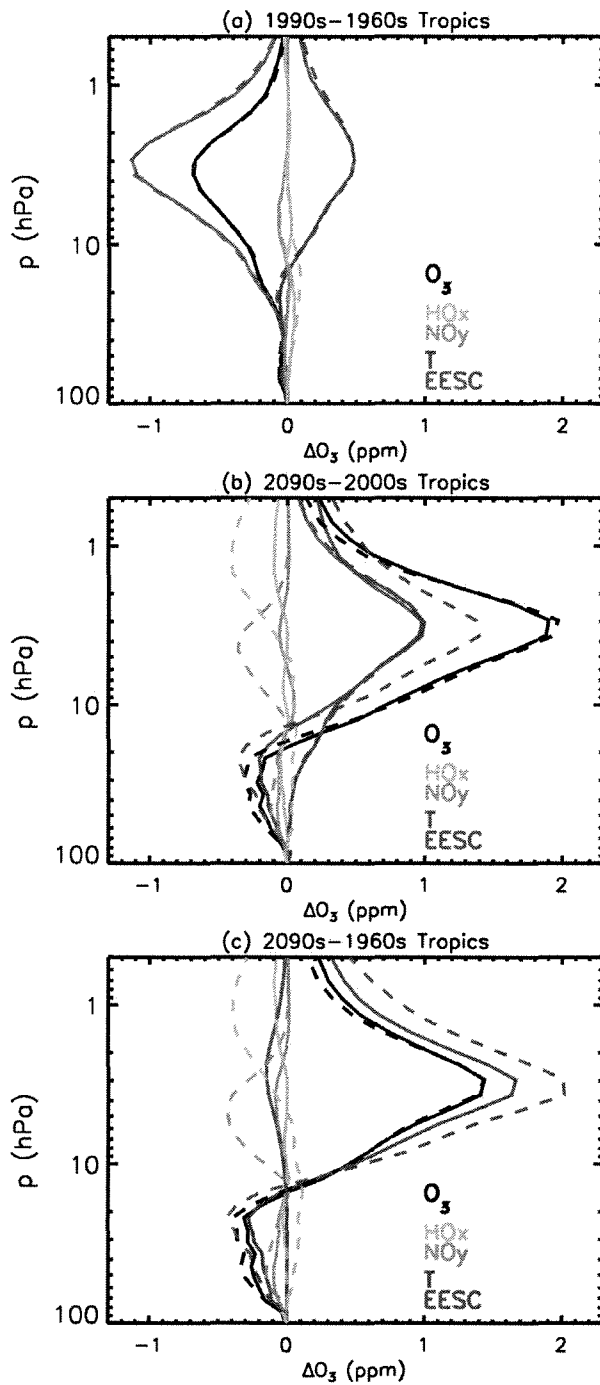
Figure 5. Vertical variation of changes in ozone (solid black curve) and individual contribution of different mechanisms for annual averages over the tropics. The changes are for (a) 1990s-1960s P1 (solid curve) and P2 (dashed curve), (b) 2090s-2000s A1b (solid curve) for A2 (dashed curve) scenario, 2090s-1960s A1b (solid curve) for A2 (dashed curve) scenario.
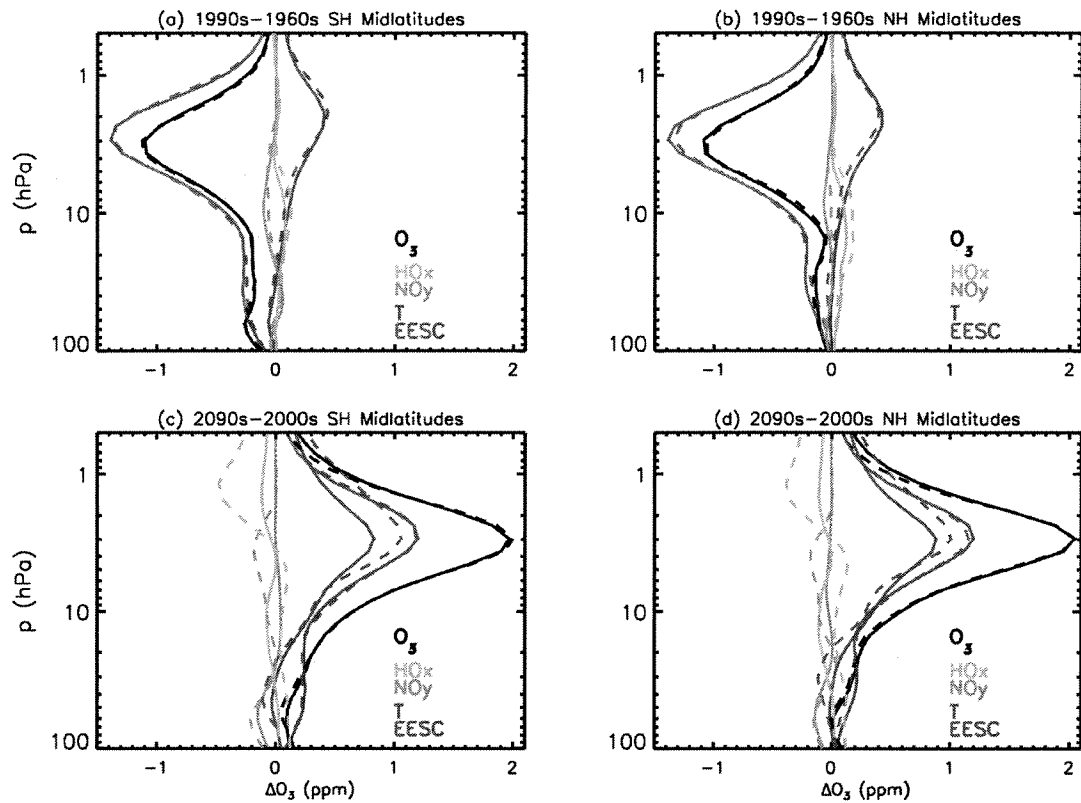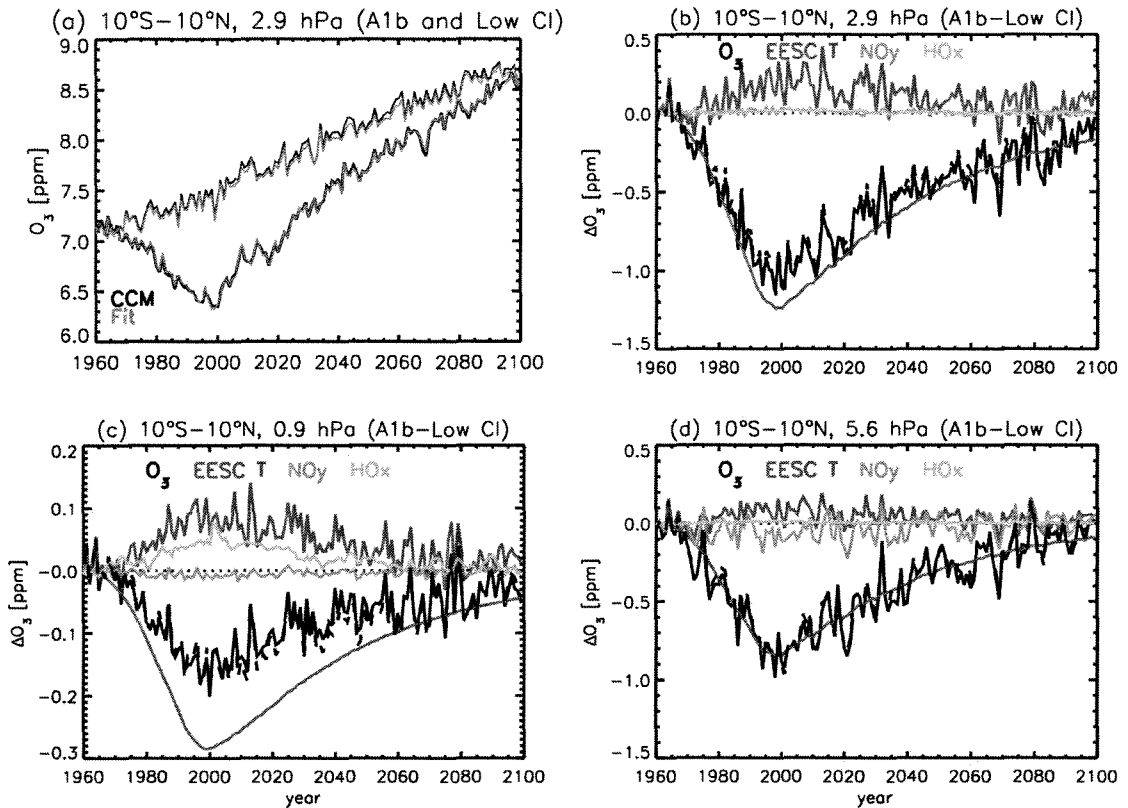
Figure 6. Sensitivities (a) of ozone to various factors (thick curves) and 3σ confidence
intervals (thin curves) for annual averages over the tropics (10°S-10°N) with the
overplotted X's showing the chemical box model calculations and the 2090s-2000s
change (b) in T, EESC, and NO_y, and HO_x divided by 100, and the contribution for A1b
(solid curves) and A2 (dashed curves).

760
761 Figure 7. Vertical variation of changes in ozone (solid black curve) and individual
762 contribution of different mechanisms for annual averages over (a,c) 50-30°S and (b,d) 30-
763 50°N. The changes are for (a,b) 1990s-1960s P1 (solid curve) and P2 (dashed curve),
764 and (c,d) 2090s-2000s A1b (solid curve) for A2 (dashed curve) scenario.
765

766
767 Figure 8. Evolution of ozone and from MLR for (a) 2.9 hPa, 10°S-10°N for A1b
768 simulation and for a fixed-halogen (Low Cl) simulation (upper curve, with the fit from
769 A1b MLR sensitivities). Difference in ozone between the A1b and fixed-halogen
770 simulation (solid black curve), and contributions due to EESC (red curve), T (blue), NO_y
771 (orange), and HO_x (green) as well as the sum of these contributions (dashed black curve)
772 for (b) 2.9 hPa, 10°S-10°N. Also shown are the individual contributions at (c) 0.9 hPa
773 (note the different scale) and (d) 5.6 hPa.